Applied Medical Informatics
Original Research Vol. 36, No. 2 /2015, pp: 31-42

Analysis of Wireless Capsule Endoscopy Images using Local Binary Patterns

Adriana Florentina CONSTANTINESCU[1], Mihaela IONESCU[2,*], Ion ROGOVEANU[3], Marius Eugen CIUREA[4], Costin Teodor STREBA[3], Vlad Florin IOVANESCU[1], Stefan Alexandru ARTENE[1], Cristin Constantin VERE[3]

[1] University of Medicine and Pharmacy of Craiova, 2-4 Petru Rares Street, Craiova, Romania.
[2] Medical Informatics Department, University of Medicine and Pharmacy of Craiova, 2-4 Petru Rares Street, Craiova, Romania.
[3] Gastroenterology Department, University of Medicine and Pharmacy of Craiova, 2-4 Petru Rares Street, Craiova, Romania.
[4] Surgery Department, University of Medicine and Pharmacy of Craiova, 2-4 Petru Rares Street, Craiova, Romania.
E-mail(*): miki.iones@yahoo.com

* Author to whom correspondence should be addressed; Tel.: +40 723 97 97 10

Received: 30 April 2015 / Accepted: 6 June 2015 / Published online: 23 June 2015

Abstract
Wireless capsule endoscopy, the gold standard in the screening and diagnosis of small bowel diseases, is one of the most recent investigations for gastrointestinal pathology. This examination has the advantages of being non-invasive, painless, with a large clinical yield, especially for small bowel diseases, but also some disadvantages. The long time necessary for reading and interpreting all frames acquired is one of these disadvantages. This inconvenient could be improved through different methods by using software applications. In this study we have used a software application for texture analysis based on local binary pattern (LBP) operator. This operator detects and removes non-informative frames in a first step, then identifies potential lesions. Our study group consisted of 33 patients from the Gastroenterology and Hepatology Centre Craiova and from the 1st Internal Medicine and Gastroenterology Clinic from the Emergency County Hospital of Craiova. The patients included in the study have corresponded to our inclusion criteria established. The exclusion criteria were represented by the contraindications of the capsule endoscopy. In the first phase of the study, we have removed the non-informative frames from the original videos obtained, and we have acquired an average reduction of 6.96% from the total number of images. In the second phase, using the same LBP operator, we have correctly identified 93.16% of telangiectasia lesions. Our study demonstrated that software applications based on LBP operator can lead to a shorter analysis time, by reducing the overall frames number, and can also provide support in diagnosis.

Keywords: Wireless capsule endoscopy; Small bowel diseases; Software applications; Local binary pattern

Introduction

Wireless capsule endoscopy (WCE) is nowadays considered the technique of choice for the screening and diagnosis of small bowel pathologies. This method allows the non-invasive study of

the entire mucosa of the small bowel, which is difficult to examine by conventional endoscopy and radiologic techniques [1-3].

Unlike conventional endoscopy, wireless capsule endoscopy is non-invasive, painless, with fewer complications for the patient and does not require sedation [1, 4]. Another advantage of wireless capsule endoscopy is represented by the large diagnostic yield of WCE for the small bowel pathologies.

The most frequent indication for the small-bowel capsule endoscopy is obscure gastrointestinal bleeding (OGIB). Other clinical indications for this investigation are represented by iron-deficiency anaemia, non stricturing small-bowel Crohn's disease, suspected / refractory or complicated celiac disease, hereditary polyposis syndromes, and small bowel tumours. Some symptoms, such as chronic unexplained abdominal pain, chronic diarrhea, significant weight loss, chronic use of non-steroidal anti-inflammatory drugs, can also be considered clinical indications for the small-bowel capsule endoscopy [4-8].

Though wireless capsule endoscopy has been established as a standard imaging technique for the small-bowel investigation, the presence of food residue, air bubbles and intraluminal fluid can impair the diagnosis and screening of the small-bowel pathology. Delayed gastric or small-bowel transit time could also represent a limitation for the visualization of the entire mucosa [5].

Another important disadvantage of the capsule endoscopy is the fact that it is a time consuming procedure. The average time required for the visualization and analysis of the acquired images, up to 55.000, ranges from 45 to 120 minutes, depending on the experience of the examiner [2, 6, 8].

The software applications developed to aid the reading and interpretation of capsule endoscopy videos could improve the required time for this step through various methods, by detecting the abnormalities such as bleedings, ulcer and polyps, digestive different organs, intestinal contractions, but also by identifying non-informative frames (frames with irrelevant content for the medical examination) [2, 9]. This study focused on the analysis of textures present within WCE images, initially to remove non-informative images and obtain a smaller number of frames to be analysed both by human physicians and software applications. Implicitly, the time spent for the analysis was shorter, for both employed methods. Subsequently, the texture analysis was employed to define and classify potential lesions present in the WCE videos.

During the past years, various methods for texture analysis were presented in literature, some of them showing great results when applied to medical images. They are mainly based on image descriptors extracted from co-occurrence matrices [10], local binary, ternary or quinary patterns [11], phase information of local Fourier or wavelet transforms [12]. LBP - Local Binary Pattern - is an extensively used operator, either in its basic form, or in enhanced variants, with multiple shapes for neighbourhood and encoding calculation, like Multivariate-LBP, Robust-LBP, Completed Robust-LBP [13] and others. This paper is based on the classic yet efficient LBP operator for detecting different textures present in WCE images.

Material and Method

Data Collection and Pre-Processing

The study group consisted of 33 subjects admitted in the 1st Internal Medicine and Gastroenterology Clinic at the Emergency County Hospital of Craiova and in the Gastroenterology and Hepatology Centre from Craiova, during 12 months. The patients included in the study group have given their informed consent and all clinical investigations have been conducted according to the principles expressed in the "Declaration of Helsinki".

The inclusion criteria were represented by the small-bowel suspected pathologies, such as occult gastrointestinal bleeding, chronic unexplained abdominal pain, chronic diarrhea, suspicion of intestinal polyp, Crohn's disease or suspected tumour pathology, with inconclusive endoscopic and serologic investigations prior the capsule ingestion. All the clinical indications were in concordance with current guidelines for small-bowel capsule endoscopy [14 – 19].

The exclusion criteria were represented by the contraindications of capsule endoscopy, such as

history of bowel obstruction, swallowing disorders, pacemaker implantation and pregnancy [4, 5].

All 33 subjects underwent small-bowel capsule endoscopy and the recording videos have been visualized and analysed also by using software applications. The patients included in the study had occult gastrointestinal bleeding, chronic unexplained abdominal pain and diarrhea and some others were already known with intestinal tumour surgery, Crohn's disease or with cancer with unknown primitive site.

Wireless capsule endoscopy system includes a swallowable device of one use, a recording device and a computer interface. The device, with a dimension of 26/11 mm and a weight of 3,7 g, contains an optic dome, a lens system, light emitting diodes (LED), the CMOS (complementary metal oxide silicone) camera module, an application specific integrated circuit (ASIC), and an antenna RFID that transmits the images to the electrodes attached to the body. The obtained images, over 50.000 images/ recording, are stored on the recording device and visualized after that on a computer interface [20-22].

Small-bowel capsule endoscopy was performed after the patients have fasted for at least 12 hours prior to capsule ingestion, and have ingested 2 l of polyethylene glycol solution. The patients were allowed to drink liquids 2 hours after the beginning of the procedure and to eat light meals after 5 hours. During the procedure we have not encountered incomplete passage incidents.

The images acquired after the procedure have been visualized and analysed by human physicians, and also by using a software application that detected similar textures within WCE images.

Image Descriptors

The main features that characterize a general image, implicitly a WCE image, may be divided in two categories: visual information and semantic information. The visual descriptors most commonly include colour, texture and shape. Semantic descriptors reflect textual data that describe various regions within an image. Right after acquisition, WCE images are only characterized by visual descriptors that may be the subject of image processing techniques. An objective descriptor for the entire WCE movie would be invariant to rotation, transformations or light level. LBP operator, proposed by Ojala et al. [23], may be used to determine and compute a texture feature within a pattern classification system, in order to discriminate between intestinal mucosa and food residues / air bubbles. LBP is a mixture of structural and statistical classification methods [24]. The basic LBP operator is based on the assumption that texture has two complementary characteristics: a pattern and its associated power [25, 26].

LBP Design and Methodology

The texture model comprised within WCE frames is determined based on a LBP code computed for each pixel of the image, after a comparison of its grey level against those of its neighbouring pixels. Thus, the original image is actually transformed in a matrix of labels, at pixel level, that represent the description of the WCE frame at a much lower scale. These labels are integer numbers and are subsequently used in image analysis.

For a circular LPB operator, the neighbourhood of a pixel is represented by a circle of radius R with the central point determined by the original pixel - now defined as the central pixel (Figure 1a). The neighbour pixels set represent a finite number P of pixels crossed by this neighbourhood and evenly spaced on this circle (Figure 1b).

Therefore, from a mathematical point of view, the notation (P, R) defines the circular neighbourhood of a pixel, where R represents the radius of the circular neighbourhood and P represents the number of pixels present on the circle with radius R. In case of a monochrome image I for which g represents the grey scale value of an arbitrary pixel (x, y), the specific local texture (1,2) is defined by the distribution of grey levels for the set of P involved neighbouring pixels present on the circumference whose centre is given by pixel (x_c, y_c):

$$T = t(g_c, g_0, g_1, ..., g_{p-1}) \quad (1)$$

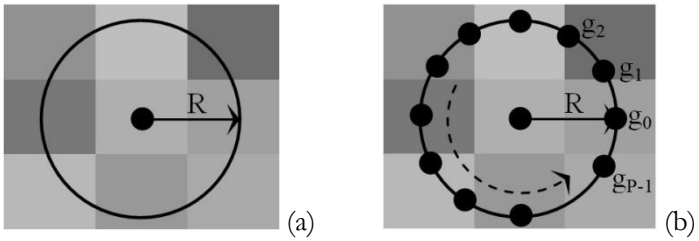

Figure 1. (a) Neighbourhood defined by a circle with radius R. **(b)** Central pixel and its P associated neighbours, circularly disposed.

The central pixel (x_c, y_c) defined in this way may comprise the characteristics of neighbouring pixels located on its circumference with radius *R*.

$$T = t(s(g_0 - g_c), s(g_{P-1} - g_c)) \tag{2}$$

With *s(x)* as the step function, the LBP operator (3) is defined as follows:

$$LBP_{P,R} = \sum_{p=0}^{P-1} s(g_p - g_c)2^p, \quad s(x) = \begin{cases} 1, x \geq 0 \\ 0, x < 0 \end{cases} \tag{3}$$

For an image *I* of size *X*Y*, its general texture is represented by a histogram *H* (4) build based on the computed LBP pattern of each pixel:

$$H(k) = \sum_{i-1}^{X} \sum_{j=1}^{Y} f(LBP_{P,R}(i,j), k), k \in [0, K] \quad f(x) = \begin{cases} 1, & x = y \\ 0, & \text{otherwise} \end{cases} \tag{4}$$

In order to simplify the computations, we may consider a central pixel g_c and its associated set of *P* neighbours g_p, $p = 0,1,...,P-1$, disposed in a circular manned and evenly spaced. Then, the difference between g_c and g_p is $d_p = g_p - g_c$. Based on these differences between the central pixel and all neighbouring pixels, the local texture may be represented by the difference vector $D = [d_0, d_1, ..., d_{P-1}]$. Due to the removal of the central pixel, *D* is robust to light changes; it is also more efficiently used in texture classification than the original image. Each local difference may be further more decomposed into two associated components:

$$d_p = s_p * m_p \quad , \quad \begin{cases} s_p = \text{sign}(d_p) \\ m_p = |d_p| \end{cases} \quad s_p = \begin{cases} 1, d_p \geq 0 \\ 0, d_p < 0 \end{cases} \tag{5}$$

In (5), s_p is considered the sign of d_p, while m_p represents the magnitude of d_p. In consequence, the difference vector $D = [d_0, d_1, ..., d_{P-1}]$ is decomposed into the sign vector $SV = [s_0, s_1, ..., s_{P-1}]$ and the magnitude vector $MV = [m_0, m_1, ..., m_{P-1}]$.

As an example, the basic LBP operator computed for a 3×3 neighbourhood considers the central pixel from the 3×3 block as the central pixel for the computations of other pixels values in the matrix.

The differences between the values of the matrix's pixels and the value of the central pixel are computed, and the values 1 or 0 are stored, corresponding to a positive or negative difference (Figure 2 a,b). The LBP code is computed after a multiplication of these results with a corresponding weight the summation of these values (results). Since each value is represented on 8 pixels (due to 8 neighbouring pixels), a total of 2^8=256 possible different labels are obtained, in accordance with the difference between grey levels of the central pixel and other pixels [24]. The LBP operator computation is repeated for each pixel in the image; then the results are stored in a vector. By the end of this operation, the final vector will contain the occurrences of the 256 labels. The histogram of LBP codes computed based on this final vector represents the texture model that represents this surface [27].

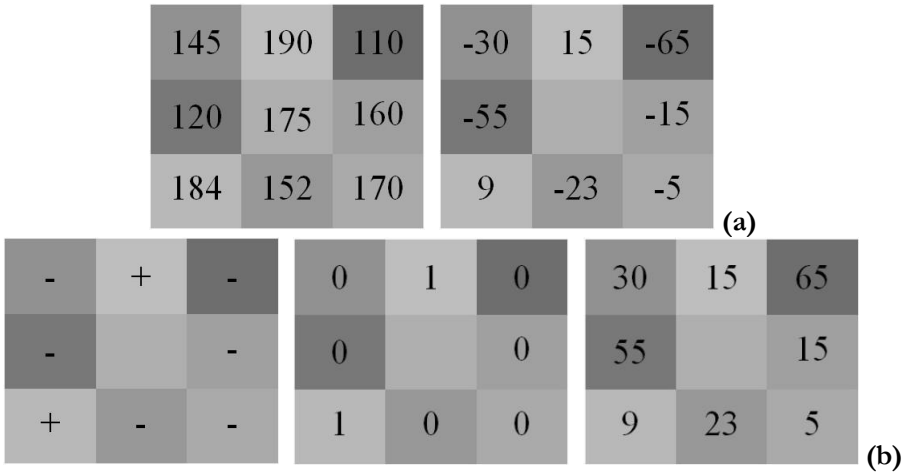

Figure 2. (a) Original 3x3 block with pixel values, next to the differences between the central pixel and the neighbouring pixels. **(b)** The sign and the magnitude matrices.

Due to the lack of control in the WCE motion, an invariant operator also robust to image rotations is needed. This aspect is accomplished using uniform patterns. The notion of pattern uniformity is defined as the number of spatial transitions present within that pattern (meaning bitwise 1/0 and 0/1 changes). The mathematical expression of pattern uniformity is given in (6):

$$U(LBP_{P,R}) = \left|s(g_{P-1} - g_c) - s(g_0 - g_c)\right| + \sum_{p=1}^{P-1}\left|s(g_p - g_c) - s(g_{P-1} - g_c)\right| \quad (6)$$

Uniform LBP patterns ($LBP_{P,R}^{u2}$) present no more than two transitions (U≤2). Patterns like 11100001 (2 bitwise transitions) or 00000011 (1 bitwise transition) are uniform, while patterns like 10001001 (4 bitwise transitions) and 10101001 (6 bitwise transitions) are not uniform. The mapping from basic LBP operator to uniform patterns implies a different label for each uniform pattern, and a single label for other patterns, thus $P*(P-1)+3$ different labels (for *P* bits) [23]. So, for a LBP with *P*=1 and *R*=8, there are 58 labels for uniform patterns, and a 59th label for the other patterns that are not uniform. The rotation invariance is obtained based on uniformity (7). The use of uniform patterns is also recommended for statistical robustness [27].

$$LBP_{P.R}^{riU2} = \begin{cases} \sum_{p=0}^{P-1} s(g_p - g_c) & U(LBP_{P,R}) \le 2 \\ P+1 & \text{otherwise} \end{cases} \quad (7)$$

In summary, LBP determines the local structure in the vicinity of a given pixel (based on a circle of radius *R* around it and *P* points on its circumference) and codes it with a unique value for each specific local structure or pattern. This operator is a preferred statistical and structural option for texture analysis, being non-linear and useful for images with different resolutions [29]. The LBP operator is one of the most employed texture descriptors, as it identifies the label that best suites its neighbourhood, encoding it as a micro-texture.

Results

The purpose of our study is to determine the measure in which texture detection using the LBP operator is useful in the classification of non-informative frames and various lesions present within WCE videos. Thus, we have divided the study into two major phases: the purpose of the first phase was to identify the optimum LBP operator that discriminates the texture of intestinal mucosa / food residues / air bubbles, then to determine the number of frames detected as non-informative

and, implicitly, the volume reduction obtained after their removal; the second phase was based on the reduced videos and reproduced the previous steps, performed this time upon normal frames (with no lesions present) and lesion frames.

The experiments relative to the first phase were performed on a set of 344 images comprising the above mentioned textures present in WCE images (Figure 3 indicates the categories of textures that comprised the first testing set). For all 344 images, we have computed several feature vectors, with different LBP operators. The LPB signatures were obtained using Matlab R2011b. The subsequent operation was the classification of these feature vectors, based on a supervised K-Means clustering technique. 67% of the images were used to determine the classifiers, the rest of 33% being used to test the precision of the classification operation with the Weka application [30]. Then, we have repeated the tests using a Support Vector Machine (SVM), for which we have used as performance indicator the area below the ROC curve (AUC). Our results are present in the following table:

Table 1. Classification results computed for various LBP operators, with different values of *R* and *P* parameters

LBP Operator	K-Means	SVM
R=1, P=8, no rotation, non-uniform patterns	82.56	0.853
R=1, P=8, rotation, non-uniform patterns	90.70	0.885
R=1, P=8, rotation, uniform patterns	93.90	0.944
R=2, P=8, no rotation, uniform patterns	89.53	0.906
R=2, P=16, rotation, uniform patterns	84.59	0.869

The results defined in Table 1 show that the best performance was obtained using a uniform LBP operator, with a neighbourhood radius of 1 and 8 pixels sampled on its circumference, for both classifiers. However, the non-uniform LBP operator with R=1 and P=8 and the uniform LBP operator with R=2 and P=8 also showed good performances (according to the chosen classifier), hence, for boosting the performance of the overall classification, a joint operator summing the scores obtained according to the SVM classification for all three above mentioned LBP operators was defined. This joint operator was subsequently used to analyse the WCE images obtained after the investigation of all 33 patients included in our study group, in order to remove those frames that presented mostly textures corresponding to food residues and air bubbles, blocking most of the intestinal mucosa captured in the image. Figure 3 presents four WCE images and their corresponding LBP histograms (the first image represents normal intestinal mucosa; in the following 2 images, the intestinal mucosa is mainly covered by food residues and debris; the fourth image contains air bubbles). There was no need for histogram normalization, since all WCE images had the same size and resolution.

In order to provide an optimum number of relevant frames to be analysed by human physicians and software applications but, in the same time, to ensure that no areas with intestinal mucosa were eliminated, we have chosen to remove all WCE images that presented less than 10% intestinal mucosa, while the rest was covered by debris and / or bubbles. This action was achieved by dividing each non-informative frame in 64 squares and performing an analysing upon each square. Subsequently, we have determined the number of non-informative frames to be removed from each WCE film included in our study group. The minimum percentage reduction was 4.28% (thus 95.72% remaining from the initial frames), while the maximum percentage reduction was 10.79% (only 89.21% remaining from the initial frames); the average reduction was 6.96% from the total number of images. Figure 4 shows a graphical representation of the total number of frames for each patient, and the associated percentage of removed images. As it may be observed, there is no correlation between the two sets of values.

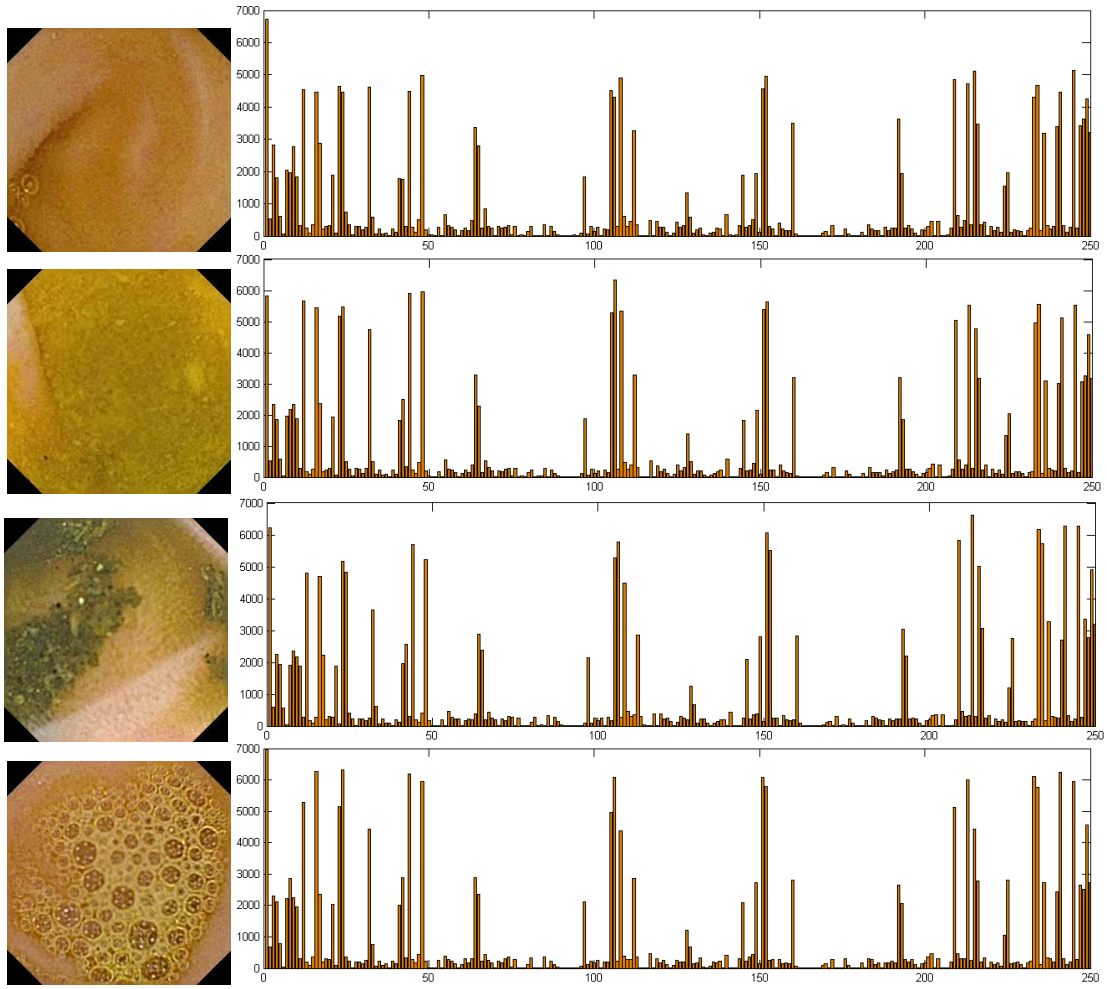

Figure 3. LBP signature for 4 WCE images (normal mucosa and food residues / air bubbles) (.jpg type images, size 288x288 pixels, type circular uniform patterns with (R=1,P=8) neighbourhood).

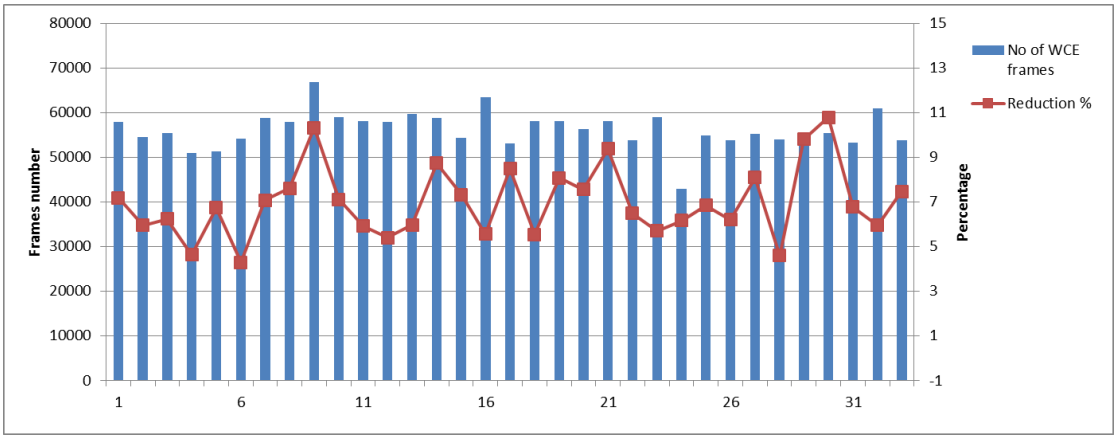

Figure 4. Reduction percentages vs. total number of frames for each patient included in the study group

During the second phase of our study, we have mainly reproduced the previous steps, with two major differences: the LBP operator was chosen to discriminate lesions present within the digestive tract of the patients included in the study group, and then the overall analysis was performed on the reduced WCE videos obtained as the result of the initial phase. Due to the small number of

patients with intestinal tumour formations, Crohn's disease and Celiac disease (Table 2), our analysis using the LBP operator was employed only for patients with telangiectasia lesions and intestinal polyps.

Intestinal polyps are benign tumours developed from the enteric mucosa. They represent small growths on the inner lining of the gut and rarely become cancerous [31]. Their main feature is the round shape, while the texture is very similar to the one of the normal intestinal mucosa. Therefore, all LBP operators showed poor results in the detection of their presence.

Telangiectasia lesions represent one of the most frequent causes of obscure gastrointestinal bleeding. They are venules or tortuous capillaries which, due to their extremely thin walls, can cause bleedings [21, 32]. Since they have a specific texture (Figure 5), the LBP operator is suitable for their detection within the global WCE image set.

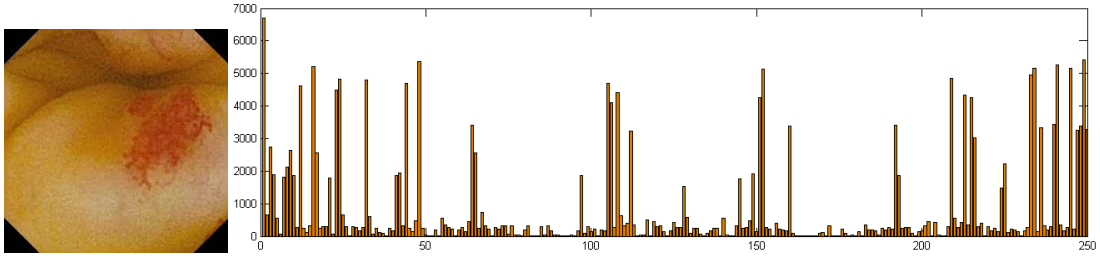

Figure 5. LBP signature for a WCE image with telangiectasia lesions.

From the reduced WCE videos, we have extracted a set of 54 images, one third containing telangiectasia lesions and the other 2 thirds representing normal intestinal mucosa. Once again, with the SVM classifier, the experiments showed that the uniform LBP operator with a neighbourhood radius of 1 and 8 pixels sampled on its circumference best discriminated between the textures present in this image set, the second best being the LBP operator with P=2 and R=8; consequently, similar to the first phase, we have used them to define a joint operator.

We have employed this joint operator for the analysis of the entire set of reduced WCE videos, obtaining a result of 93.16% correct telangiectasia lesions detection (SVM AUC was 0.924).

Table 2. Distribution of lesion types within the study group

Diagnostic	Number of patients	AUC
Telangiectasia	9	0.924
Intestinal polyps	6	<0.150
Celiac disease	2	-
Crohn's disease	1	-
Intestinal tumoral formation	1	-

Discussion

Food residues, debris, air bubbles are best identified by their specific texture, making it suitable for LBP analysis. Moreover, LPB is an image descriptor invariant to light changes, which is the case of WCE frames. The light needed to acquire proper images is provided by the 6 LEDs located circularly in the capsule's dome. However, the capsule is not always positioned perpendicularly to the intestinal wall, most of the times facing in fact the intestinal lumen. Therefore, the light distribution is uneven throughout the WCE image dataset, the regions close to the capsule being more illuminated than the areas located farther away from it [33].

LBP is frequently used in the medical imaging field, due to its structural and statistical data comprised in histograms. It has provided good results in multiple applications of image processing, being employed to determine specific textures within mammography, magnetic resonance or

endoscopy images [34-36].

Our study proved that LBP is also suitable for texture analysis in WCE images, allowing both a reduction of the total number of images to be analysed, and also an automatic detection of telangiectasia lesions.

Time reduction in the analysis of WCE videos may be quantitative and qualitative. The time reduction in the quantitative analysis of WCE videos is mainly performed by removing two types of frames: non-informative frames (either containing debris, bubbles, or presenting too much or too little light), and duplicate frames (when the speed of the capsule is very low compared to the acquisition rate, thus the video contains sequences of successive almost identical frames). In both cases, it is useful to remove those frames before performing a thorough image analysis, in order to reduce the overall time spent on the video analysis. Obviously, the number of reduced frames is dependent of the content and context of the patient's digestive tract and it may only be statistically enclosed within specific margins. It also depends on the notion of "irrelevant content" for WCE frames and the measure in which debris and bubbles cover the mucosa. In our study, we have chosen a minimum of 10% visible intestinal mucosa, obtaining thus an average reduction of 6.96% of the images to be analysed both by physicians and software applications specific for lesion detection. A greater threshold value would lead to a bigger number of frames removed from the final WCE videos, but it would also increase the chances to miss a potential lesion present in the small area of visible mucosa. In this direction, our future research is focused on the following idea: remove entirely the frames with less than 10% visible intestinal mucosa, and for all other frames, remove only the irrelevant content leaving the mucosa, in order to interfere as much as possible with the lesion detection process.

Conclusion

Automatic lesion detection is a process that would help physicians reduce the time spent for the WCE images analysis, by indicating specific sections that contain potential lesions. There are various processing techniques that either detect or enhance certain properties of an image, thus being more precise than the human eye. For very small lesions, or incompletely captured within in a frame, or present in a small number of images, so for this type of lesions that may be missed by a human examiner, software applications prove very efficient in their detection, increasing the accuracy of the diagnosis. In our study, we have obtained good results in performing the automatic detection of telangiectasia lesions. Since they are characterized by a specific texture, the LBP operator was an optimum choice. In this direction, our future research is focused on adding a colour detection component that would further more increase the accuracy of automatic lesion detection.

List of abbreviations

Wireless capsule endoscopy (WCE)
Local Binary Pattern (LBP)
Support Vector Machine (SVM)

Conflict of Interest

The authors declare that they have no conflict of interest.

Acknowledgements

This paper was published under the frame of European Social Found, Human Resources

Development Operational Programme 2007 - 2013, project no. POSDRU/159/1.5/S/136893.

References

1. Romero-Vázquez J, Argüelles-Arias F, García-Montes JM, Caunedo-Álvarez Á, Pellicer-Bautista FJ, Herrerías-Gutiérrez JM. Capsule endoscopy in patients refusing conventional endoscopy. World J Gastroenterol 2014;20(23):7424-7433.
2. Iakovidis DK, Tsevas S, Polydorou A. Reduction of capsule endoscopy reading times by unsupervised image mining. Comput Med Imaging Graph 2010;34(6):471-478.
3. Aktas H, Mensink PB. Small bowel diagnostics: current place of small bowel endoscopy. Best Pract Res Clin Gastroenterol 2012;26(3):209-220.
4. Kopylov U, Seidman EG. Clinical applications of small bowel capsule endoscopy. Clin Exp Gastroenterol 2013;6:129-137.
5. Ladas SD, Triantafyllou K, Spada C, Riccioni ME, Rey JF, Niv Y, et al. European Society of Gastrointestinal Endoscopy (ESGE): recommendations (2009) on clinical use of video capsule endoscopy to investigate small-bowel, esophageal and colonic diseases. Endoscopy 2010;42(3):220-227.
6. Koulaouzidis A, Rondonotti E, Karargyris A. Small-bowel capsule endoscopy: a ten-point contemporary review. World J Gastroenterol 2013;19(24):3726-3746.
7. Bardan E, Nadler M, Chowers Y, Fidder H, Bar-Meir S. Capsule endoscopy for the evaluation of patients with chronic abdominal pain. Endoscopy 2003;35(8):688-689.
8. Gheorghe C, Iacob R, Bancila I. Olympus capsule endoscopy for small bowel examination. J Gastrointestin Liver Dis 2007;16(3):309-313.
9. Mackiewicz M. Capsule Endoscopy - State of the Technology and Computer Vision Tools after the First Decade. New Techniques in Gastrointestinal Endoscopy, Prof. OliviuPascu (Ed.), ISBN: 978-953-307-777-2, InTech, 2011.
10. Nanni L, Brahnam S, Ghidoni S, Menegatti E, Barrier T. Different Approaches for Extracting Information from the Co-Occurrence Matrix. PLoS ONE 2013;8(12):e83554.
11. Paci M, Nanni L, Lahti A, Aalto-Setala K, Hyttinen J, Severi S. Non-Binary Coding for Texture Descriptors in Sub-Cellular and Stem Cell Image Classification. Curr Bioinforma 2013;8:208-219.
12. Rahtua E, Heikkiläa J, Ojansivub V, Ahonen T. Local phase quantization for blur-insensitive image analysis. Image Vis Comput 2012;8:501-512.
13. Zhaoa Y, Jiac W, Huc RX, Min H. Completed robust local binary pattern for texture classification. Neurocomputing 2013;106:68-76.
14. Pennazio M, Santucci R, Rondonotti E, Abbiati C, Beccari G, Rossini FP, DeFranchis R. Outcome of patients with obscure gastrointestinal bleeding after capsule endoscopy: report of 100 consecutive cases. Gastroenterology 2004;126(3):643-653.
15. Herrerías JM, Caunedo A, Rodríguez-Téllez M, Pellicer F, Herrerías JM Jr. Capsule endoscopy in patients with suspected Crohn's disease and negative endoscopy. Endoscopy 2003;35(7):564-568.
16. Tatar EL, Shen, EH, Palance AL, Sun JH, Pitchumoni CS. Clinical utility of wireless capsule endoscopy: experience with 200 cases. J Clin Gastroenterol 2006;40(2):140-144.
17. Vere CC, Cazacu S, Streba CT, Sima F, Parvu DC, Ionescu A. Capsule endoscopy: Diagnostic Role in Obscure Gastrointestinal Bleeding. Curr Health Sci J 2009;39(3):154-158.
18. Katsinelos P, Lazaraki G, Gkagkalis A, Gatopoulou A, Patsavela S, Varitimiadis K, et al. The role of capsule endoscopy in the evaluation and treatment of obscure-overt gastrointestinal

bleeding during daily clinical practice: a prospective multicenter study. Scand J Gastroenterol 2014;49(7):862-870.
19. Xue M, Chen X, Shi L, Si J, Wang L, Chen S. Small-bowel capsule endoscopy in patients with unexplained chronic abdominal pain: a systematic review. Gastrointest Endosc 2015;81(1):186-193.
20. Neumann H, Fry LC, Nägel A, Neurath MF. Wireless capsule endoscopy of the small intestine: a review with future directions. Curr Opin Gastroenterol 2014;30(5):463-471.
21. Vere CC. Tehnici moderne de diagnostic şi tratament în patologia organică a intestinului subţire. Ed. Medicală Universitară Craiova, 2010.
22. Vere CC, Foarfa C, Streba CT, Cazacu S, Parvu D, Ciurea T. Videocapsule endoscopy and single balloon enteroscopy: novel diagnostic techniques in small bowel pathology. Rom J Morphol Embryol 2009;50(3):467-474.
23. Ojala T, Pietikäinen M, Mäenpää T. Multiresolution gray-scale and rotation invariant texture classification with local binary patterns. IEEE Trans Pattern Anal Mach Intell 2002;24(7):971-987.
24. Ojala T, Pietikäinen M, Harwood D. A comparative study of texture measures with classification based on feature distributions. Pattern Recognit 1996;29(1):51-59.
25. Maenpaa T. The Local Binary Pattern Approach to Texture Analysis - Extensions and Applications. Infotech Oulu and Department of Electrical and Information Engineering. University of Oulu. Finland, 2003.
26. Mäenpää T, Pietikäinen M, Ojala T. Texture Classification by Multi-Predicate Local Binary Pattern Operators. ICPR 15th International Conference on Pattern Recognition (ICPR'00), 2000;3:3951.
27. Mdakane L, Van den Bergh F. Extended local binary pattern features for improving settlement type classification of quickbird images. In: PRASA 2012: Twenty-Third Annual Symposium of the Pattern Recognition Association of South Africa, Pretoria, South Africa, 29-30 November 2012.
28. Heikkilä M, Pietikäinen M. A texture-based method for modeling the background and detecting moving objects. IEEE Trans Pattern Anal Mach Intell 2006;28(4):657-662.
29. García-Olalla O, Alegre E, Fernández-Robles L, García-Ordás MT, García-Ordás D. Adaptive local binary pattern with oriented standard deviation (ALBPS) for texture classification. EURASIP J Image Video Process 2013;2013:31.
30. Hall M, Frank E, Holmes G, Phahringer B, Reutemann P, Witten IH. The WEKA Data Mining Software: An Update. SIGKDD Explorations 2009;11(1):10-18.
31. Huang A, Summers RM, Hara AK. Surface curvature estimation for automatic colonic polyp detection. Proc. SPIE 5746. Medical Imaging 2005: Physiology, Function, and Structure from Medical Images. 393 (April 19, 2005).
32. Gunjan D, Sharma V, Rana SS, Bhasin DK. Small bowel bleeding: a comprehensive review. Gastroenterol Rep (Oxf) 2014;2(4):262-275.
33. Lau PY, Correia PL. Detection of bleeding patterns in WCE video using multiple features. Conf Proc IEEE Eng Med Biol Soc 2007;2007:5601-5604.
34. Oliver A, Lladó X, Freixenet J, Martí J. False positive reduction in mammographic mass detection using local binary patterns. Med Image Comput Comput Assist Interv 2007;10 (Pt1):286-293.
35. Sørensen L, Shaker SB, de Bruijne M. Texture classification in lung CT using local binary patterns. Med Image Comput Comput Assist Interv 2008;11(Pt 1):934-941.

36. Nanni L, Lumini A, Brahnam S. Survey on LBP based texture descriptors for image classification. Expert Syst Appl 2012;39(3):3634-3641.